Quality Improvement Study

Medicine®

OPEN

The altered Granger causality connection among pain-related brain networks in migraine

Yanzhe Ning, MD[a,b], Ruwen Zheng, MD[c], Kuangshi Li, MD[d], Yong Zhang, MD[a], Diyang Lyu, MM[b], Hongxiao Jia, PhD[b], Yi Ren, PhD[a,*], Yihuai Zou, PhD[a,*]

Abstract

Numerous fMRI studies have confirmed functional abnormalities in resting-state brain networks in migraine patients. However, few studies focusing on causal relationships of pain-related brain networks in migraine have been conducted. This study aims to explore the difference of Granger causality connection among pain-related brain networks in migraine without aura (MWoA) patients.

Twenty two MWoA patients and 17 matched healthy subjects were recruited to undergo resting-state fMRI scanning. Independent component analysis was used to extract pain-related brain networks, and Granger causality analysis to characterize the difference of Granger causality connection among pain-related brain networks was employed.

Seven pain-related brain networks were identified, and MwoA patients showed more complex Granger causality connections in comparison with healthy subjects. Two-sample t test results displayed that there was the significant difference between right-frontoparietal network (RFPN) and executive control network (ECN).

This study indicates that the specific intrinsic brain Granger causality connectivity among pain-related networks in MwoA patients are affected after long-term migraine attacks.

Abbreviations: BIC = Bayesian information criterion, DMN = default mode network, ECN= executive control network, FC= functional connectivity, fMRI = functional magnetic resonance, GCA = Granger causality analysis, GPDC = generalized partial directed coherence, ICA = independent component analysis, MwoA = migraine without aura, RFPN = right-frontoparietal network, ROI = regions of interest, SMN = sensorimotor network, SN = salience network, VN = visual network.

Keywords: Granger causality analysis, migraine, pain-related networks, resting-state functional magnetic resonance imaging

1. Introduction

Migraine, a chronic neurological disorder, has brought great attention from the public due to its high prevalence and large medical burden, according to the Global Burden of Disease (GBD 2010).[1,2] For migraine patients, the quality of daily life is seriously influenced by the repeated migraine attacks and its ubiquitous sleep disorders. For children, attachment styles, maternal personality profile, and motor coordination impairment are affected by migraine.[3–5] Thus, to study the neural mechanisms of migraine is of great importance.

In the past decades, with the fast development of functional magnetic resonance imaging (fMRI), it has opened a window to explore the pathogenesis of neurological disorders. Significant improvements have been made in the field of researches on the mechanisms of diseases, such as stroke,[6] Alzheimer's disease,[7] depression,[8] knee osteoarthritis,[9] and so on. Recently, it has also been applied in migraine to explore the changes of intrinsic brain activity after long-term pain attacks.[10,11] In the aspect of whole brain, amplitude of low frequency fluctuations and graph theory were used to investigate the change of spontaneous neural activity after long-term pain attacks.[12,13] As for regional resting-state networks, previous studies demonstrated that migraine without aura (MwoA) patients had the abnormal functional connectivity within the default mode network (DMN),[14] executive control network (ECN),[15] sensorimotor network (SMN),[16]salience network (SN),[17,18] periaqueductal gray network,[19] and right-frontoparietal network (RFPN).[20] The DMN, RFPN, ECN, and left-frontoparietal network (LFPN) are related to cognition, and potentially associated with pain processing. As the insula is core

Editor: Helen Gharaei.

YN and RZ contributed equally to this work.

Authors' contributions: YZN, RWZ, YR, and YHZ conceived and designed the study. YZN and KSL analyzed the data. YZN, DYL, YZ, HXJ, and ZJT performed the experiment. YZN, RWZ, YR, and YHZ drafted the manuscript and gave final approval of the manuscript.

This paper is supported by the National Natural Science Foundation of China (Grant no. 81473667), the Middle-aged Teachers Research Funds of Beijing University of Chinese Medicine (Grant no. 2017-JYB-JS072), the Young Scientist Development Program of Dongzhimen Hospital Affiliated to Beijing University of Chinese Medicine (DZMYS-201605), and the Beijing Young Talent Program of Beijing Education Committee (Grant no.YETP0823).

The authors have no conflicts of interest to disclose.

[a] Department of Neurology and Stroke Center, Dongzhimen Hospital, the First Affiliated Hospital of Beijing University of Chinese Medicine, [b] The National Clinical Research Center for Mental Disorders & Beijing Key Laboratory of Mental Disorders, Beijing Anding Hospital, Capital Medical University, [c] Department of Acupuncture and Moxibustion, Dongfang Hospital, The Second Affiliated Hospital of Beijing University of Chinese Medicine, [d] Department of Internal Medicine, Gulou Hospital of Traditional Chinese Medicine of Beijing.

[*] Correspondence: Yi Ren and Yihuai Zou, Department of Neurology and Stroke Center, Dongzhimen Hospital, the First Affiliated Hospital of Beijing University of Chinese Medicine, Beijing, 100700, China (e-mails: rywendy1982@sina.com; zouyihuai2004@163.com).

Medicine (2018) 97:10(e0102)

Received: 18 October 2017 / Received in final form: 24 November 2017 / Accepted: 13 February 2018

http://dx.doi.org/10.1097/MD.0000000000010102

regions of the SN, SN is also assumed to play a vital role in processing pain.[21] Both the visual network (VN) and SMN are afferent sensory networks which are related to pain transmission.

In the study of causal relationships among brain networks, the causality model is suitable to display intranetwork communications. The Granger causality analysis (GCA) is always applied in studying causalities among brain regions or networks.[22] It has been widely used in researches on stroke,[23] Alzheimer's disease,[24] and so on. Wang et al[25] investigated the casual patterns of bilateral posterior thalamus with the rest of the brain in migraine patients by applying GCA, which found disrupted effective connection pathways between the posterior thalamus and other pain-related cortical or subcortical regions. However, to our knowledge, there is few study focused on causal relationships of pain-related brain networks in MwoA patients.

In this study, we extracted pain-related brain networks (DMN, SMN, SN, ECN, RFPN, LFPN, and VN) by using independent component analysis (ICA), and applied the multivariate Granger model to analyze the intranetwork causality in MwoA patients. We postulated that there were 2 different causal connectivity patterns in MwoA patients and healthy subjects, and significant alterations in the 7 important pain-related brain networks (DMN, SMN, SN, ECN, RFPN, LFPN, and VN) of MwoA patients in comparison with healthy subjects.

2. Materials and methods

This study was approved by the Dongzhimen Hospital of Beijing Ethics Committee. All subjects signed informed consents before inclusion in this study.

2.1. Participants

Twenty two right-handed subjects (3 males, aged 27.50 ± 5.90 years) were diagnosed as MwoA according to the classification criteria of the International Headache Society[26] and met the criteria below: from 18 to 45 years old; at least 2 migraine attacks per month in the last 3 months; with at least one-year history of migraine; with no history of prophylactic or therapeutic medicine in the past 3 months; with no history of long-term use of analgesics; The exclusion criteria were as follows: other types of migraine; with history of dysmenorrhea or other chronic paining disease; with history of drug or alcohol abuse; any MRI contraindications. Another 17 healthy subjects (4 males, aged 27.18 ± 4.69 years) were recruited with no history of migraine and other neurologic disorders.

2.2. MRI acquisition

Images were acquired using a 3.0 Tesla MRI scanner (Siemens, Sonata Germany) at Dongzhimen Hospital, Beijing, China. Prior to scanning, all participants were asked to rest for 20 minutes and were instructed to stay still, think of nothing in particular, keep eyes closed, and not to fall asleep during scanning. Earplugs were worn to attenuate scanner noise and foam head holders were immobilized to minimize head movements during scanning.

Prior to the functional scanning, we collected high-resolution structural information for anatomical localization by using 3D MRI sequences. The resting-state fMRI data were collected using a single-shot, gradient-recalled echo-planar imaging sequence with the following parameters: repetition time = 2000 ms, echo time = 30 ms, flip angle = 90°, matrix = 64×64, field of view = 225 mm × 225 mm, slice thickness = 3.5 mm, gap = 1 mm, 32 interleaved axial slices, and 180 volumes.

2.3. Experimental paradigm

In the current research, we employed a 490-second resting scan first, and then 250-second high-resolution structural scan.

2.4. Data processing

The data preprocessing was conducted by software Data Processing Assistant for Resting-State fMRI (DPARSF, http://rfmri.org/DPARSF). A total of 231 volumes for each subject were corrected for slice timing after the first 10 volumes were discarded for signal equilibrium. The slice timing and head movement were corrected for the residual phase sequence data. No subject was excluded due to excessive motion (translation > 2 mm or rotation $> 2°$). Functional imaging of each subject was performed based on the standardized diffeomorphic anatomical registration. The image data were normalized into the Montreal Neurological Institute (MNI) template, resampled into 3 mm × 3 mm × 3 mm, temporal band pass filtering at 0.01 to 0.1 Hz, and smoothed with a Gaussian kernel of 4 mm full width at half-maximum. Linear trends were removed from the time courses, and 8-parameter nuisance signal extraction. Finally, 9 nuisance signals (global mean, white matter, and cerebrospinal fluid signals and 6 motion parameters) were regressed out.

Independent component analysis (ICA) used the Group ICA of fMRI Toolbox (GIFT, http://mialab.mrn.org/software/gift/). After 20 times randlnit and bootstrap and regression operations, we extracted 7 resting-state networks from 3 components, which were SN, DMN, ECN, RFPN, LFPN, SMN, and VN.

Functional network connectivity (FNC, http://mialab.mrn.org/software/fnc) software was applied to analyze network causal relationships. Seven resting-state network components were selected and filtered at 0.01 to 0.10 Hz and the generalized partial directed coherence (GPDC) was selected as the measured parameter. GPDC is a linear frequency-domain quantifier of the multivariate relationship between simultaneously observed time series, which is applied in functional connectivity inference.[27] Detailed introductions of the GPDC could be referred in previous paper.[28]

Between the 0.01 an d0.1 Hz bandwidth, the multivariate Granger model estimation was utilized. Using group level optimization from the Bayesian information criterion (BIC), the order of the model was estimated. To compare the intervention group before treatment with the control group, *P*-values were set as .05 for group comparisons. The results were corrected by false discovery rate (FDR) for multiple comparisons and final results were displayed onto a 3D standard brain surface using BrainNet Viewer.

3. Results

3.1. Demographic and clinical Information

Demographic and psychiatric characteristics of all subjects were displayed in Table 1.

Compared with healthy subjects, MwoA patients showed no significant differences in age and educational level ($z = -0.68$, $P = .50$, for age), ($z = -1.36$, $P = .17$, for educational level). The duration of migraine ranged from 12 to 180 months (mean value, 87.55 ± 64.88 months). Frequency of migraine attacks varied from 2 to 8 times/month (mean value, 3.77 ± 1.74 times/month). Visual analog scale scores ranged from 3 to 8 (mean value, 5.59 ± 1.68).

Table 1

The demographic and clinical information of MWoA patients and healthy controls.

Items	Healthy controls (N = 17)	MWoA patients (N = 22)
Gender (male/female)	4/13	3/19
Age, years	27.18 ± 4.69*	27.50 ± 5.90
migraine history, months	–	87.55 ± 64.88
Educational level, years	17.35 ± 1.06*	17.14 ± 0.64
Frequency of migraine attacks, times/month	–	3.77 ± 1.74
VAS scores	–	5.59 ± 1.68

MwoA = migraine without aura, VAS = visual analog scale.

* Results from 2-sample nonparametric test of the comparison between MWoA patients and healthy controls, $z = -0.68$ $P = .50$ (for age), $z = -1.36$, $P = .17$ (for educational level).

3.2. ICA results

Applying ICA in all subjects, the SN, DMN, ECN, RFPN, LFPN, SMN, and VN are extracted. Spatial positional distributions of the 7 pain-related resting-state networks are shown in Figure 1 and Table 2.

3.3. GCA results

The Granger causality of the 7 pain-related resting-state brain networks in MwoA patients showed different patterns of causal connections compared with healthy subjects. MwoA patients showed more complex Granger causality connections. For the patients, RFPN and ECN were the core networks with more effective connections than others, while LFPN, VN, and ECN comprised the hubs of causal connection in healthy subjects (Fig. 2, left and center panels). Moreover, one-sample *t* test results showed that for patients, RFPN was the hub inputting information from other networks, and ECN was the hub mainly outputting information from other networks, while the RFPN and ECN were quiet opposite for healthy subjects. Two-sample *t* test results displayed that there was the significant difference between RFPN and ECN ($P < .0015$, corrected by FDR, Fig. 2, right panels).

4. Discussion

In the present study, we tried to investigate the difference of Granger causality connection among pain-related brain networks between MwoA patients and healthy subjects. Our results revealed that MwoA patients showed more complex Granger causality connections among pain-related brain networks than healthy subjects. More importantly, we found that only 1 significant causal relation from ECN to RFPN was observed in comparison with healthy subjects.

Resting-state networks reflect spontaneous fluctuations in the brain with the subject at rest, which could be detected by fMRI.[29] Numerous researches have revealed FC abnormalities in MwoA patients, which mainly covered the pain-processing networks.[30] Neuroimaging reviews also indicated that abnormalities of pain-related resting-state networks were caused by long-term ongoing pain attacks, and positively correlated with the duration of migraine.[31,32] In the present study, we extracted 7 resting-state networks, which had been demonstrated to be related with pain processing. They were divided into afferent sensory networks and cognitive implementation networks. Afferent sensory networks mainly involved in pain transmission, while cognitive implementation networks mainly participated in pain processing. We also applied the GCA to detect causal

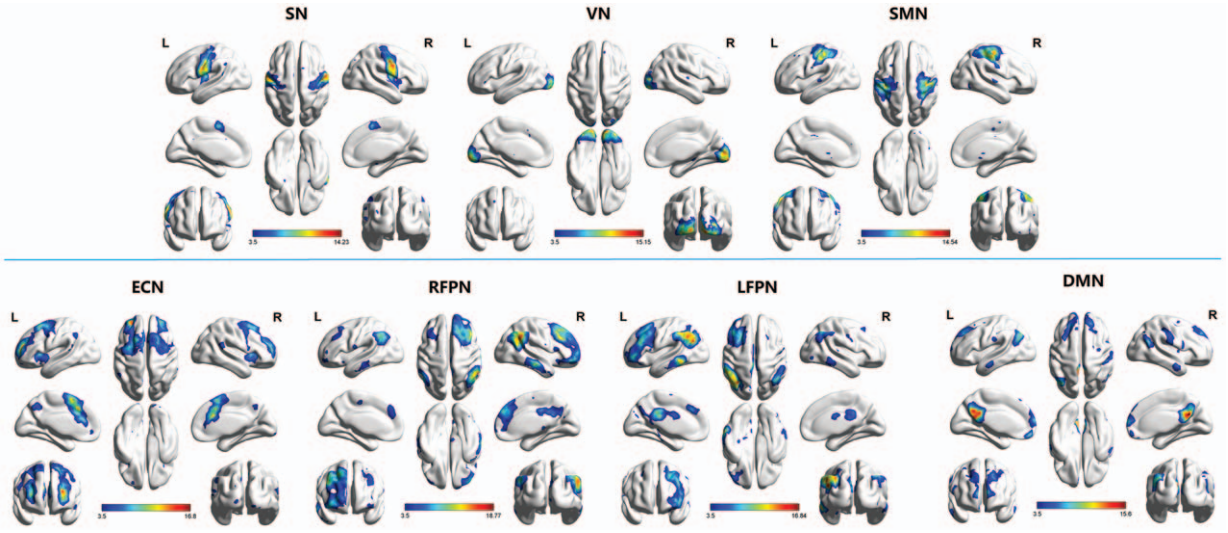

Figure 1. Pain-related networks screened through ICA. One-sample t test of pain-related networks of all 39 participants projected onto ICBM-152 brain surface template, as identified through ICA, including sensorimotor network (SMN), visual network (VN), default mode network (DMN), executive control network (ECN), salience network (SN), left-frontoparietal network (LFPN), and right-frontoparietal network (RFPN). The *t* value (depicted by cold to warm colors) represents the spatial statistical significance of the current networks. DMN = default mode network, ECN = executive control network, L = left, LFPN = left-frontoparietal network, R = right, RFPN = right-frontoparietal network, SMN = sensorimotor network, SN = salience network, VN = visual network.

Table 2

Spatial positional distributions of brain networks.

	Brodmann areas	Voxels (L/R)	Maximum *t* values (L/R) and coordinates
Salience network			
Insula	13	59/77	8.5 (−36,−11,9)/9.8 (36,−8,9)
Superior temporal gyrus	22,38	103/70	9.6 (−59,−11,6)/10.2 (62,−5,9)
Precentral gyrus	3,4,6,13,43,44	537/611	13.0 (−45,−13,31)/14.2 (45,−7,34)
Inferior frontal gyrus	6,9,44,45,47	27/79	8.5 (−59,4,19)/11.6 (53,1,19)
Middle frontal gyrus	6,9	–/26*	–/6.7 (53,2,39)*
Postcentral gyrus	1,2,3,4,40,43	309/124	12.4 (−50,−8,20)/10.2 (59,−8,20)
Visual network			
Fusiform gyrus	18,19	41/22	9.5 (−18,−88,−11)/7.3 (21,−82,−14)
Inferior occipital gyrus	17,18,19	104/88	12.3 (−30,−88,−3)/14.3 (27,−88,−3)
Lingual gyrus	17,18	287/279	12.2 (−9,−94,−5)/14.8 (18,−87,4)
Middle occipital gyrus	18,19	157/192	11.7 (−27,90,5)/15.1 (21,−90,7)
Cuneus	17,18,30	169/234	14.1 (−15,−96,0)/14.7 (21,−87,7)
Somatomotor network			
Sub-gyral	6,7,40	55/163	8.3 (−39,−30,46)/5.5 (33,−35,63)
Precentral gyrus	4,6	259/371	11.3 (−36,−21,54)/13.0 (42,−15,50)
Inferior parietal lobule	2,40	165/99	14.5 (−50,−27,46)/10.3 (42,−35,52)
Middle frontal gyrus	6	22/74	7.2 (−27,−6,56)/8.3 (30,−9,58)
Postcentral gyrus	1,2,3,4,5,40	353/355	13.4 (−50,−24,45)/12.1 (50,−18,42)
Executive control network			
Sub-gyral	6,10	126/92	8.5 (−24,44,12)/8.1 (24,47,11)
Insula	13	85/–*	10.0 (−33,18,2)/–*
Superior temporal gyrus	22,38	60/–*	11.6 (−45,8,-5)/–*
Inferior frontal gyrus	9,45,47	87/17	11.0 (−45,14,−6)/5.5 (50,10,33)
Anterior cingulate	24,32,33	119/91	10.2 (−3,27,24)/14.6 (3,30,21)
Precentral gyrus	6	37/–*	7.2 (−27,-6,50)/–*
Cingulate gyrus	24,32	153/122	16.8 (−3,22,35)/14.7 (6,25,26)
Middle frontal gyrus	6,8,9,10	660/462	15.2 (−27,47,17)/11.3 (30,53,8)
Superior frontal gyrus	6,8,9,10,11	445/465	15.0 (−27,50,14)/12.9 (3,14,49)
Medial frontal gyrus	6,8,9,32	142/99	14.3 (−3,11,46)/14.0 (3,14,46)
Right frontoparietal network			
Precuneus	7,31	–/88*	10.3 (6,−68,34)/–*
Inferior parietal lobule	7,39,40	116/342	12.6 (−53,−53,39)/16.2 (48,−47,41)
Supramarginal gyrus	40	99/207	12.1 (−53,−54,36)/17.7 (53,−51,22)
Angular gyrus	39,40	52/71	12.8 (−53,−56,36)/13.7 (45,−57,30)
Superior temporal gyrus	22,39	45/139	9.5 (−48,−54,28)/18.8 (53,−54,28)
Superior parietal lobule	7	–/29*	–/8.8 (39,−56,50)*
Medial frontal gyrus	6,8,9,10,11,32	62/778	11.9 (−3,45,31)/13.8 (42,28,29)
Superior frontal gyrus	6,8,9,10,11	–/750*	–/13.1 (24,25,43)*
Precentral gyrus	9	–/25*	–/13.0 (42,25,37)*
Anterior cingulate	10,32,42	–/79*	–/12.8 (3,39,15)*
Sub-gyral	10	–/82*	–/9.3 (18,28,40)*
Middle temporal gyrus	20,21	–/198*	–/13.7 (65,−15,−14)*
Inferior temporal gyrus	20,21	–/66*	–/11.6 (62,−21,−17)*
Left frontoparietal network			
Inferior temporal gyrus	20,21,37	66/–*	13.2 (−59,−47,−10) /–*
Middle temporal gyrus	20,21,37	154/–*	12.8 (−59,−47,−8)/–*
Sub-gyral	8	115/–*	10.2 (−42,41,−2)/–*
Inferior frontal gyrus	9,10,44,45,46,47	203/–*	9.7 (−45,44,−2)/–*
Middle frontal gyrus	6,8,9,10,11,46,47	842/–*	11.7 (−45,33,20)/–*
Superior frontal gyrus	6,8,9,10,11	145/–*	9.0 (−24,20,49)/–*
Middle temporal gyrus	39	130/–*	15.0 (−48,−66,28) /–*
Superior temporal gyrus	39	68/–*	10.3 (−50,−57,25) /–*
Angular gyrus	39	109/38	15.8 (−45,−65,31)/8.2 (42,−62,36)
Supramarginal gyrus	40	192/–*	13.7 (−50,−54,36)/–*
Inferior parietal lobule	7,39,40	378/192	16.1 (−33,−62,42)/10.7 (42,−56,44)
Precuneus	7,19,39	123/–*	16.8 (−30,−65,42)/–*
Superior parietal lobule	7	66/–*	14.7 (−33,−65,45)/–*
Cingulate gyrus	23,31	121/49	12.7 (−3,−33,32)/9.0 (3,−36,32)
Default mode network			
Superior frontal gyrus	8,9,10	104/*	8.9 (−21,40,39)/–*
Medial frontal gyrus	9,10,11	133/98*	11.1 (−3,55,−13)/10.9 (3,62,8)
Posterior cingulate	23,29,30,31	118/117*	16.7 (−3,−48,25)/25.7 (3,−54,25)
Cingulate gyrus	23,31	102/59*	20.0 (−3,−54,28)/22.0 (3,−54,28)
Precuneus	7,23,31	209/147	19.0 (−3,−54,30)/15.6 (3,−57,30)
Middle temporal gyrus	39	76/–*	10.3 (−48,−63,28)/–*
Inferior parietal lobule	7,39,40	35/–*	9.2 (−42,−68,39)/–*
Angular gyrus	39	60/–*	10.1 (−42,−65,36)/–*
Superior temporal gyrus	39	37/–*	6.4 (−48,−60,20) /–*

L = left, R = right.

* No activated voxels on the left or right.

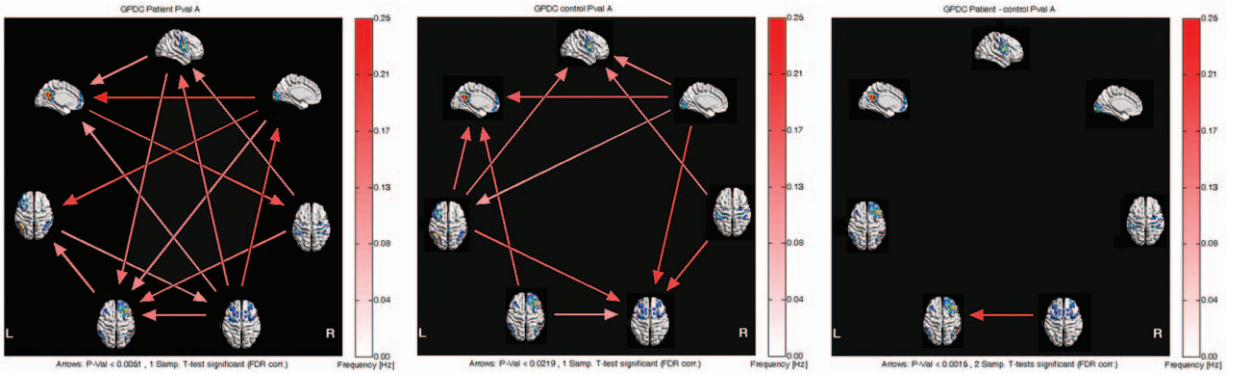

Figure 2. Inter- and intragroup comparisons of MwoA patients and healthy subjects. (A) one-sample *t* test result of intergroup intranetwork causal relationship of MwoA patients. (B) One-sample *t* test result of intergroup intranetwork causal relationship of healthy subjects. (C) Two-sample *t* test result of intragroup intranetwork causal relationship of MwoA patients minus healthy subjects. Panels represent visual descriptions of causal connectivity between 2 networks among the 7 resting-state networks, including sensorimotor network (SMN), visual network (VN), default mode network (DMN), executive control network (ECN), salience network (SN), left-frontoparietal network (LFPN), and right-frontoparietal network (RFPN). Arrow directions represent cause and effect. Values on the color bar (corresponding with arrow colors) demonstrate frequency at which causality was found. DMN = default mode network, ECN = executive control network, ICA = independent component analysis, L = left, LFPN = left-frontoparietal network, MwoA = migraine without aura, R = right, RFPN = right-frontoparietal network, SMN = sensorimotor network, SN = salience network, VN = visual network.

influence and flow of information among the 7 resting-state networks. An interesting finding was that MwoA patients showed more complex causal connections than healthy subjects, which was in line with other chronic paining diseases, such as chronic neck pain.[33] We speculated that the altered Granger causality connection among pain-related networks for MwoA patients was associated with nociceptive signals induced by frequent migraine attacks.

Another finding was that the flows of information for RFPN and ECN in MwoA patients were completely opposite to healthy subjects. Moreover, in comparison with healthy subjects, patients showed the significant difference in causal connections between RFPN and ECN. As known to all, the ECN plays an important role in cognitive processing for working memory and attention, which mainly covers dorsolateral prefrontal cortex (DLPFC).[34] DMN is considered as the key component in top-down modulation functions on the cognitive and sensory aspects of psychological activities.[35] Meanwhile the RFPN is involved in cognitive control and top-down modulation.[36] It is confirmed that the ECN acts as a feasible modulator between DMN and RFPN,[37] which involves the cognitive control over both emotional and nonemotional materials.[38] Previous studies had revealed that there were abnormalities among DMN, ECN and RFPN in chronic pain diseases. An investigation of patients with persistent somatoform pain disorder found that compared with healthy subjects, patients showed decreased functional network connectivities (FNCs) between SMN and VN, between DMN and ECN and between SN and ECN as well as RFPN, and increased FNCs between SMN and LFPN.[39] Xue et al. reported that MwoA patients had greater intrinsic connectivity between the DMN and ECN, and the greater connectivity is associated with the duration of migraine attacks. In contrast to these studies, the present study showed that the causal relation between ECN and RFPN was opposite in MwoA patients and control subjects, which suggested that an abnormal feedback between ECN and RFPN, and certainly affects pain processing in migraine.

As it is reported, chronic pain is a strong disruptor of intranetwork FC within the DMN, SN, RFPN, and ECN.[14,15,17,20] These GCA findings suggest that brain functional networks may be performed interactively in encoding different aspects of pain. We speculate that these effects of MwoA on the functional networks may reveal the underlying neural mechanism that pain can be modulated by important causal links in cognitive networks.

There were also several limitations for the interpretation of the current results. Firstly, our results were only limited to MwoA patients, and it was unclear about other subtype patterns of migraine. Secondly, as a preliminary study, the sample size was small. This could be the reason that the periaqueductal gray network was not extracted by applying ICA, which could modulate pain perception.[40] Further studies with larger sample size are needed in the future.

5. Conclusion

Our findings may provide new insights into the characterization of intrinsic causality connection among pain-related networks in migraine. Moreover, the change in Granger causality connection between RFPN and ECN may serve as a new potential biomarker for migraine.

References

[1] Stovner LJ, Hagen K. Prevalence, burden, and cost of headache disorders. Curr Opin Neurol 2006;19:281–5.
[2] Leonardi M, Raggi A. Burden of migraine: international perspectives. Neurol Sci 2013;34(suppl 1):S117–118.
[3] Esposito M, Parisi L, Gallai B, et al. Attachment styles in children affected by migraine without aura. Neuropsychiatr Dis Treat 2013;9:1513–9.
[4] Esposito M, Roccella M, Gallai B, et al. Maternal personality profile of children affected by migraine. Neuropsychiatr Dis Treat 2013;9:1351–8.
[5] Esposito M, Verrotti A, Gimigliano F, et al. Motor coordination impairment and migraine in children: a new comorbidity? Eur J Pediatr 2012;171:1599–604.
[6] Liu J, Qin W, Zhang J, et al. Enhanced interhemispheric functional connectivity compensates for anatomical connection damages in subcortical stroke. Stroke 2015;46:1045–51.
[7] Barrett FS, Workman CI, Sair HI, et al. Association between serotonin denervation and resting-state functional connectivity in mild cognitive impairment. Hum Brain Mapp 2017; doi: 10.1002/hbm.23595. [Epub ahead of print].
[8] Steffens DC, Wang L, Manning KJ, et al. Negative affectivity, aging, and depression: results from the Neurobiology of Late-Life Depression (NBOLD) Study. Am J Geriatr Psychiatry 2017;25:1135–49.

[9] Chen X, Spaeth RB, Freeman SG, et al. The modulation effect of longitudinal acupuncture on resting state functional connectivity in knee osteoarthritis patients. Mol Pain 2015;11:67.
[10] Amin FM, Hougaard A, Magon S, et al. Altered thalamic connectivity during spontaneous attacks of migraine without aura: a resting-state fMRI study. Cephalalgia 2017; doi: 10.1177/0333102417729113. [Epub ahead of print].
[11] Coppola G, Di Renzo A, Tinelli E, et al. Thalamo-cortical network activity during spontaneous migraine attacks. Neurology 2016;87:2154–60.
[12] Ning YZ, Li KS, Zhang Y, et al. Effect of acupuncture at Zulinqi (GB41) on the amplitude of low frequency fluctuations in migraine without aura patients: a resting-state functional magnetic resonance imaging study. Int J Clin Exp Med 2017;10:3038–48.
[13] Liu J, Zhao L, Lei F, et al. Disrupted resting-state functional connectivity and its changing trend in migraine suffers. Hum Brain Mapp 2015;36:1892–907.
[14] Tessitore A, Russo A, Giordano A, et al. Disrupted default mode network connectivity in migraine without aura. J Headache Pain 2013;14:89.
[15] Russo A, Tessitore A, Giordano A, et al. Executive resting-state network connectivity in migraine without aura. Cephalalgia 2012;32:1041–8.
[16] Zhang J, Su J, Wang M, et al. The sensorimotor network dysfunction in migraineurs without aura: a resting-state fMRI study. J Neurol 2017;264:654–63.
[17] Amin FM, Hougaard A, Magon S, et al. Change in brain network connectivity during PACAP38-induced migraine attacks: a resting-state functional MRI study. Neurology 2016;86:180–7.
[18] Xue T, Yuan K, Zhao L, et al. Intrinsic brain network abnormalities in migraines without aura revealed in resting-state fMRI. PLoS One 2012;7: e52927.
[19] Mainero C, Boshyan J, Hadjikhani N. Altered functional magnetic resonance imaging resting-state connectivity in periaqueductal gray networks in migraine. Ann Neurol 2011;70:838–45.
[20] Li Z, Lan L, Zeng F, et al. The altered right frontoparietal network functional connectivity in migraine and the modulation effect of treatment. Cephalalgia 2017;37:161–76.
[21] Legrain V, Iannetti GD, Plaghki L, et al. The pain matrix reloaded: a salience detection system for the body. Prog Neurobiol 2011;93:111–24.
[22] Barnett L, Seth AK. The MVGC multivariate Granger causality toolbox: a new approach to Granger-causal inference. J Neurosci Methods 2014;223:50–68.
[23] Zhao Z, Wang X, Fan M, et al. Altered effective connectivity of the primary motor cortex in stroke: a resting-state fMRI study with Granger causality analysis. PLoS One 2016;11:e0166210.
[24] Chen Y, Yan H, Han Z, et al. Functional activity and connectivity differences of five resting-state networks in patients with Alzheimer's disease or mild cognitive impairment. Curr Alzheimer Res 2016;13:234–42.
[25] Wang T, Chen N, Zhan W, et al. Altered effective connectivity of posterior thalamus in migraine with cutaneous allodynia: a resting-state fMRI study with Granger causality analysis. J Headache Pain 2015;17:17.
[26] Headache Classification Committee of the International Headache SocietyThe International Classification of Headache Disorders, 3rd edition (beta version). Cephalalgia 2013;33:629–808.
[27] Baccala LA, Sameshima K. Partial directed coherence: a new concept in neural structure determination. Biol Cybern 2001;84: 463–74.
[28] Havlicek M, Jan J, Brazdil M, et al. Dynamic Granger causality based on Kalman filter for evaluation of functional network connectivity in fMRI data. Neuroimage 2010;53:65–77.
[29] Biswal B, Yetkin FZ, Haughton VM, et al. Functional connectivity in the motor cortex of resting human brain using echo-planar MRI. Magn Reson Med 1995;34:537–41.
[30] Colombo B, Rocca MA, Messina R, et al. Resting-state fMRI functional connectivity: a new perspective to evaluate pain modulation in migraine? Neurological Sci 2015;36(suppl 1):41–5.
[31] Schwedt TJ, Dodick DW. Advanced neuroimaging of migraine. Lancet Neurol 2009;8:560–8.
[32] Schwedt TJ, Chiang CC, Chong CD, et al. Functional MRI of migraine. Lancet Neurol 2015;14:81–91.
[33] Zhang H, Chen H, Wang H, et al. Effect of Chinese tuina massage therapy on resting state brain functional network of patients with chronic neck pain. J Trad Chin Med Sci 2015;2:60–8.
[34] Seeley WW, Menon V, Schatzberg AF, et al. Dissociable intrinsic connectivity networks for salience processing and executive control. J Neurosci 2007;27:2349–56.
[35] Liao W, Mantini D, Zhang Z, et al. Evaluating the effective connectivity of resting state networks using conditional Granger causality. Biol Cybern 2010;102:57–69.
[36] Corbetta M, Shulman GL. Control of goal-directed and stimulus-driven attention in the brain. Nat Rev Neurosci 2002;3:201–15.
[37] Jiang L, Xu T, He Y, et al. Toward neurobiological characterization of functional homogeneity in the human cortex: regional variation, morphological association and functional covariance network organization. Brain Struct Funct 2015;220:2485–507.
[38] Ochsner KN, Gross JJ. The cognitive control of emotion. Trends Cogn Sci 2005;9:242–9.
[39] Zhao Z, Huang T, Tang C, et al. Altered resting-state intra- and inter-network functional connectivity in patients with persistent somatoform pain disorder. PLoS One 2017;12:e0176494.
[40] Fields H. State-dependent opioid control of pain. Nat Rev Neurosci 2004;5:565–75.